Available online at www.sciencedirect.com

SciVerse ScienceDirect

Ceramics International 39 (2013) 5443–5451

CERAMICS INTERNATIONAL

www.elsevier.com/locate/ceramint

Adsorptive removal of Congo red dye from wastewater by mixed iron oxide–alumina nanocomposites

A. Mahapatra, B.G. Mishra, G. Hota*

Department of Chemistry, NIT Rourkela, Orissa 769008, India

Received 30 November 2012; received in revised form 3 December 2012; accepted 15 December 2012
Available online 26 December 2012

Abstract

Nanocomposites composed of mixed iron and aluminium oxide (Fe_2O_3–Al_2O_3), have been synthesized by hydrothermal method, and further used as adsorbent for the adsorptive decolorization of Congo red dye from an aqueous system. The as-prepared nanomaterials were sintered at 500 °C and 1000 °C, to obtain pure Fe_2O_3–Al_2O_3 mixed composites. The XRD studies confirmed the formation of pure and crystalline FeOOH–AlOOH (as-prepared), γ-Fe_2O_3–Al_2O_3 at 500 °C and α-Fe_2O_3–Al_2O_3 phases at 1000 °C. The morphology and size of the obtained nanocomposites were characterized by SEM and TEM. Effects of pH, contact time, initial concentration of adsorbate have been studied. The optimum pH for maximum removal of Congo red in all the three phases of nanocomposites was found to be 7. The maximum removal capacity was 498 mg/g for γ-Fe_2O_3–Al_2O_3 phases. Among the three different adsorbents, γ-Fe_2O_3–Al_2O_3 shows complete removal within 15 min of contact time.

Keywords: Nanocomposites; Hydrothermal method; Congo red; Adsorbent

1. Introduction

Composites where nanoscale inclusions are imbedded within matrix of a material have attracted increasing research attention in recent years. Nanocomposites refer to materials consisting of at least two phases with one dispersed in another that is called matrix and thus forms a three dimensional network [1]. Nanocomposites exhibit properties different from that of the bulk material. A small inclusion of nano sized particle produces a great change in the properties [2]. As the nano-scale morphology plays an important role in achieving desired macroscopic properties, it is important to characterize the interaction of the nanoscale samples with the intrinsically immiscible phases [3]. Nanocomposite with fine uniform domains is challenging because we need to control both the micro structural length scales as well as the elemental distributions. Now-a-days, researchers are much more interested in mixed metal oxide nanoparticle because of its broad class of catalytic, electronic, magnetic properties and also for its heterogeneous catalysis [4]. Recently, Dong et al., have synthesized iron oxide and alumina nanocomposite (Fe_2O_3–Al_2O_3) with a unique structure, which shows a remarkable catalytic performance in Fischer–Tropsch synthesis [5]. These nanoparticles often exhibit superior properties and performance; it is because of its large specific surface area. Among various metal oxides the oxides of aluminium (Al) and iron (Fe) have large advantages because of their low cost, extensive availability, thermal stability and remarkable adsorption capacity [6,7]. Violante et al. have studied on the adsorption of heavy metal ions on mixed Fe–Al oxides in absence or presence of increasing concentrations of oxalate or tartrate [8]. Ground water and surface water pollution is a serious problem due to its high toxicity for the presence of dyes and organic waste. Among them Congo red dye is an important source of water pollution and a known human carcinogen. Congo red dye is a benzidine-based azo dye with a complex chemical structure and is highly soluble in aqueous solution. It is generated from textiles, printing and dyeing, paper, rubber, plastics

*Corresponding author. Tel.: +6612462655.
E-mail addresses: garud31@yahoo.com, garud@nitrkl.ac.in (G. Hota).

0272-8842/$ - see front matter © 2012 Elsevier Ltd and Techna Group S.r.l. All rights reserved.
http://dx.doi.org/10.1016/j.ceramint.2012.12.052

industries etc [9]. Therefore, it is very important to remove the remaining Congo red before it mixed up with any water resource. Structural stability of Congo red is the major challenge for its removal from wastewater treatment [10]. Different process have been used to remove Congo red from colored effluents but among all, adsorption has been recognized as the most popular treatment process due to its simplicity, high efficiency, easy recovery and the reusability of the adsorbent [11–13]. Similarly, Gong et al., studied the removal of cationic dyes from aqueous solution using magnetic multi-wall composite carbon nanotube as adsorbent. Adsorption characteristics of the nanocomposite adsorbent were examined using methylene blue, neutral red and brilliant cresyl blue as adsorbates [14].

In the present study, iron oxide–alumina mixed nanocomposite was prepared by hydrothermal method and their adsorption characteristic for the removal of Congo red dye from aqueous solution was studied. The synthesized mixed oxy-hydroxide sample was sintered at different temperatures to obtain mixed oxides nanocomposites. The adsorption experiments such as effect of contact time, pH, adsorbent dose and initial concentration variation were explored in batch experiments. The adsorption isotherm and kinetic studies were also carried out to elucidate the adsorption mechanism. A comparative study for maximum removal capacity of using different mixed oxide nanocomposite adsorbents was also reported here.

2. Experimental section

2.1. Materials

Ferrous sulphate ($FeSO_4 \cdot 7H_2O$) and Aluminium nitrate (Al $(NO_3)_3 \cdot 9H_2O$) of analytical grade with purity 99.0% was obtained from Merck, India. Both NaOH pellets and NH_3 solution were also obtained from Merck, India. All chemicals were used without further purifications. Double distilled water was used throughout the experiments for preparation and dilution of the solutions.

2.2. Synthesis of Fe_2O_3–Al_2O_3 nanocomposites

In this work, Fe_2O_3–Al_2O_3 nanocomposites were prepared by hydrothermal method. The Al $(NO_3)_3 \cdot 9H_2O$ and $FeSO_4 \cdot 7H_2O$ salts were taken in a molar ratio of 1:1 and were mixed in 50 mL distilled water. Then the mixed solution was stirred vigorously. At the same time, a mixed precipitant was prepared by adding 25 mL of 2 M NH_3 solution into 25 mL of NaOH solution so as to maintain a ratio of 1:1. The mixed precipitant was added drop wise to above mixture solution with vigorous stirring. Simultaneously, the pH of the solution was measured using pH meter. At pH 5.6 green precipitate was formed. The formation of precipitate in the whole mixture solution was transferred into a 100 mL Teflon cupped pressure pot. The pressure pot was sealed and kept in an electric oven at 180 °C for 6 h. After that the pressure pot was cooled at room temperature and the resultant product was centrifuged, washed with deionised water several times and dried at 50 °C for 5–6 h followed by grinding. The obtained deep yellow powder was further calcined at 500 °C and 1000 °C, to form mixed Fe_2O_3–Al_2O_3 nanocomposite.

2.3. Characterization

The surface morphology of iron oxide–alumina mixed nanocomposite was characterized by using a SEM JEOL JSM- 5300 and was operated at 15 kV. In order to increase the conductivity of the samples, they were gold coated using a JEOL FRC 1200 fine coater before taking SEM. The powder X-ray diffraction patterns were obtained on a Pan analytical X-ray diffractometer (PW1830) using Cu K_α ($\lambda = 1.541$ Å) radiation. A JEOL 200 HRTEM was used to characterize the iron oxide–alumina mixed nanocomposite materials and was operated at 200 kV. The mixed nanocomposites were dispersed in ethanol and then a drop of the above dispersion was taken on a carbon coated copper grid (300 meshes) for HR-TEM imaging. A digital pH meter (Satorius Model PB-11) combined with glass electrode was used for all experiments. A Shimadzu UV–visible spectrophotometer (Shimadzu-2450) was used for adsorption study of Congo red dye.

2.4. Adsorption experiments for Congo red dye by batch process

The un sintered and sintered mixed iron oxide–alumina nanocomposites samples were used as adsorbent for removal of organic dye pollutants. The adsorption study was carried out by taking 100 mg of powder samples into 10 mL of Congo red ($C_{32}H_{22}N_6O_6S_2Na_2$) solution (100 mg/L) under stirring condition. The adsorption study was carried out with change in different parameters viz. change in time, pH, and initial concentration of Congo red. After appropriate time of stirring, the solution was filtered using whatman-40 filter paper, and finally analyzed by UV–visible spectrophotometer.

3. Result and discussion

3.1. Structural properties

We have used hydrothermal method for preparation of iron–aluminium oxide mixed nanocomposites powder. The obtained powder was sintered at different temperatures and the formation of different phases was confirmed by XRD study. Fig. 1 shows the XRD pattern of iron oxide–alumina mixed nanocomposites. This result revealed that the formed materials are crystalline in nature. Fig. 1(a) shows XRD pattern of the as prepared mixed nanocomposites. It is observed from the XRD data that the hydrothermal mediated synthesis of as prepared samples consists of mixture of boehmite (γ-AlOOH) and lepidocrocite (γ-FeOOH) phases, which is confirmed from the JCPDS Files (File no.84-0175) and (File no. 77-0247),

respectively. The obtained mixed oxy hydroxide phases of iron–aluminium nanocomposite was sintered at 500 °C and 1000 °C in air for 2 h. Fig. 1(b) and (c) represent the XRD pattern of iron oxide–alumina nanocomposites obtained on sintering the as prepared mixed oxy-hydroxide at 500 °C and 1000 °C, respectively. It is also observed from the XRD data that the sintered sample contains the mixture of Iron and Aluminum oxides. The 2θ values of mixed oxides formed after sintering the sample at 500 °C found to match with (JCPDS File no 89-8104) and (JCPDS File no 29-0062), this result confirmed the formation of mixed γ-Fe_2O_3–Al_2O_3 nanocomposites. Similarly, the formation of mixed α-Fe_2O_3–Al_2O_3 phase was obtained after sintering the as-prepared sample at 1000 °C, which was confirmed from XRD pattern (Fig. 1(c)).

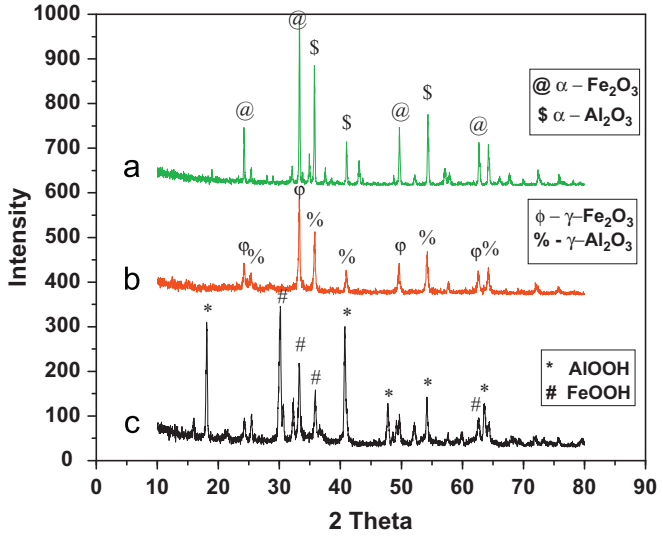

Fig. 1. XRD data of (a) unsintered mixed oxy-hydroxide nanocomposite, (b) mixed oxide sintered at 500 °C, (c) mixed oxide sintered at 1000 °C.

The surface morphology of Iron-Alumina oxide mixed nanocomposites has been studied by scanning electron microscopy method. Fig. 2 represents the SEM and EDAX analysis of mixed nanocomposites obtained by hydrothermal synthesis of as-prepared and sintered samples. It is observed from the SEM images that the as-prepared samples (Fig. 2(a)) are rod shaped and are in the size range of 100–300 nm. It is also observed that the rod like morphology of mixed nanocomposites is retained after sintering the as prepared samples at higher temperature. The presence of Fe, Al and O elements in the mixed composite were confirmed by the EDAX spectrum (Fig. 2(d)).

In order to obtain more information about the formation, morphology and dimensions of mixed oxide nanocomposite, we have carried out the HRTEM imaging. Fig. 3(a) shows the HRTEM micrograph of Fe_2O_3–Al_2O_3 mixed oxide nanocomposite sintered at 500 °C. It was observed from the HRTEM imaging that the nanoparticle formed were not having uniform size; instead a size range from 100–300 nm was found. Fig. 3(b) shows the selected area diffraction pattern of mixed oxide nanocomposites. The corresponding diffraction rings and bright spot on the electron diffraction pattern indicate the formation of highly crystalline Fe_2O_3–Al_2O_3 mixed oxide nanocomposite, which is also consistent with XRD results.

3.2. UV-adsorption spectroscopy analysis

Fig. 4(a) shows the UV–vis absorption spectrum of iron-alumina mixed oxide nanocomposite prepared by

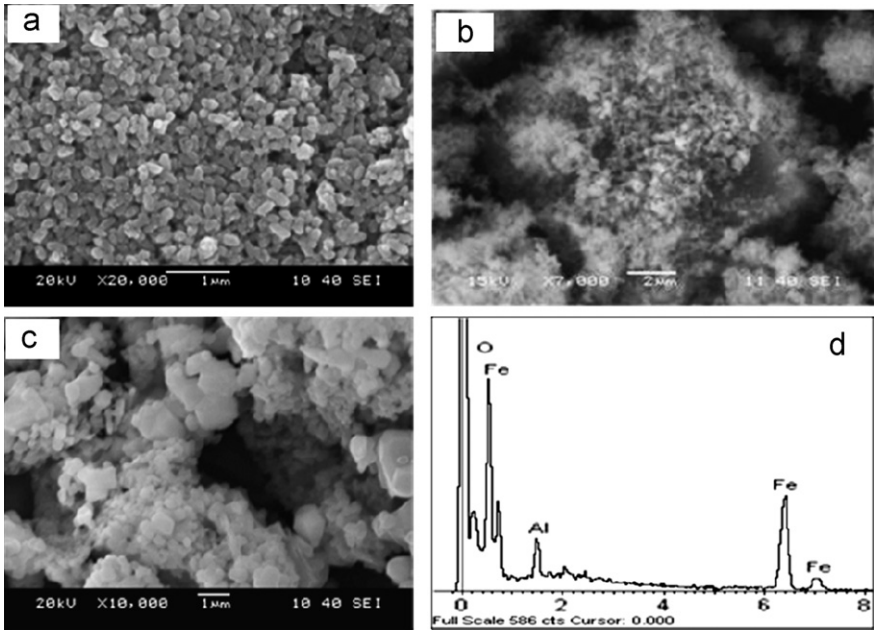

Fig. 2. SEM image of (a) mixed FeOOH and AlOOH nanocomposite, (b) mixed γ-Fe_2O_3 and γ-Al_2O_3 nanocomposite sintered at 500 °C, (c) mixed α-Fe_2O_3 and α-Al_2O_3 sintered at 1000 °C, (d) EDAX image of mixed iron oxide and alumina nanocomposites.

hydrothermal method and sintered at different temperatures. Optical band gap is also. measured using UV–vis spectra analysis. The spectral absorption coefficient, α, is defined as

$$\alpha(\lambda) = 4\pi k(\lambda)/\lambda$$

where $k(\lambda)$ is the spectral extinction coefficient obtained from the absorption curve and λ is the wavelength. The band gap, E_g, is obtained by fitting the experiment absorption data with the following equation

$$(\alpha hv)^2 = A(hv - E_g)$$

where hv is the photon energy, α is the adsorption coefficient, E_g is the band gap, and A is a characteristic parameter independent of photon energy. The value of band gap E_g has been obtained from the intercept of the extrapolated linear part of the $(\alpha hv)^2$ versus hν curve with the energy (hv) axis [15,16]. The band gap for mixed oxy hydroxide nanocomposite is 1.9 eV, for gamma phase the band gap is 1.7 eV and the alpha phase mixed oxide nanocomposite has band gap value 1.95 eV as shown in Fig. 4(b). The value of band gap shows that all of the mixed oxide nanocomposites are semiconductor in nature even after sintering at different temperature.

3.3. Adsorption study of Congo red by mixed nanocomposites

The FeOOH–AlOOH and Fe_2O_3–Al_2O_3 mixed nanocomposites prepared by hydrothermal synthesis method has been used for removal of Congo red dye from aqueous solutions. We had carried out the adsorption process by batch experiments using 25 mL of neat and cleaned capped glass bottles. The colour photograph of Congo red dye molecules before and after adsorption studies using both un-sintered (FeOOH–AlOOH) and sintered (Fe_2O_3–Al_2O_3) mixed nanocomposite materials are shown in Fig. 5.

3.3.1. Effect of pH on adsorption of Congo red dye

The pH values of dye solutions affect the chemistry of both the dye molecules and the adsorbent materials. Simultaneously, the pH of dye solution plays an important role in the whole adsorption process and also on the adsorption capacity. Original pH of Congo red solution (100 mg/L) is about 7.5. It was seen that the dye solution changes its color from red to dark blue when pH was adjusted in highly acidic range and becomes dark blue in highly basic range i.e., pH 9 and above [17,18]. Therefore,

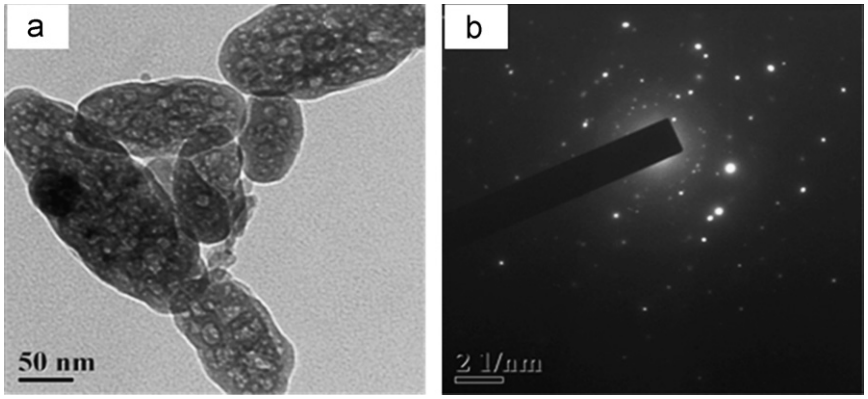

Fig. 3. HRTEM image of (a) mixed γ-Fe_2O_3 and γ-Al_2O_3 nanocomposite sintered at 500 °C, and (b) SAED image of mixed oxide nanocomposite.

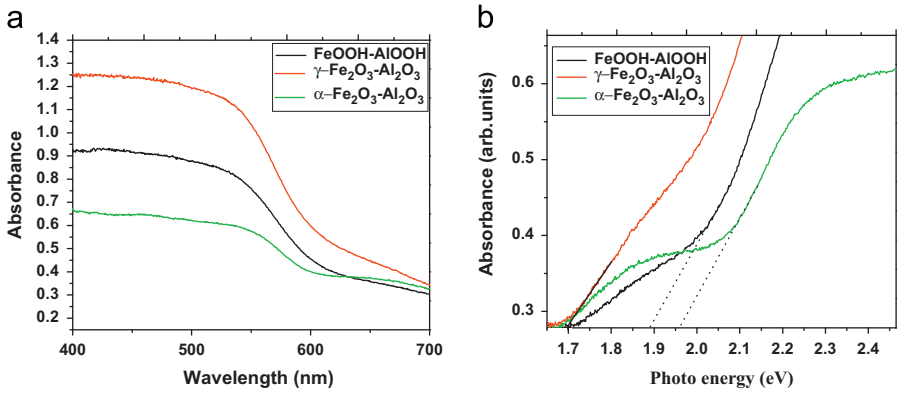

Fig. 4. UV- analysis of (a) mixed FeOOH and AlOOH nanocomposite, mixed γ-Fe_2O_3 and γ-Al_2O_3 nanocomposite sintered at 500 °C, mixed α-Fe_2O_3 and α-Al_2O_3 sintered at 1000 °C, (b) Optical property of all the samples.

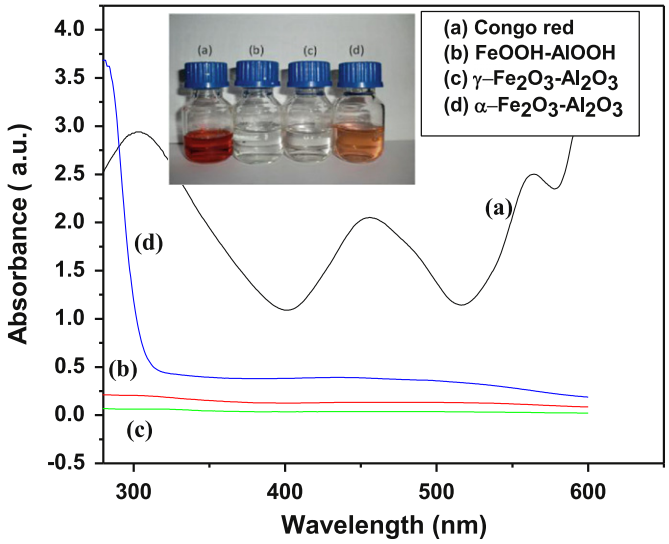

Fig. 5. UV–vis absorption spectra of Congo red solution and after being treated by three different samples, the initial concentration of Congo red are 100 mg/L. (a) Before adsorption, after adsorption by 0.1 gm (b) un-sintered, (c) sintered at 500 °C and (d) sintered at 1000 °C mixed Iron oxide and alumina nanocomposite, in 15 mins at pH 7.

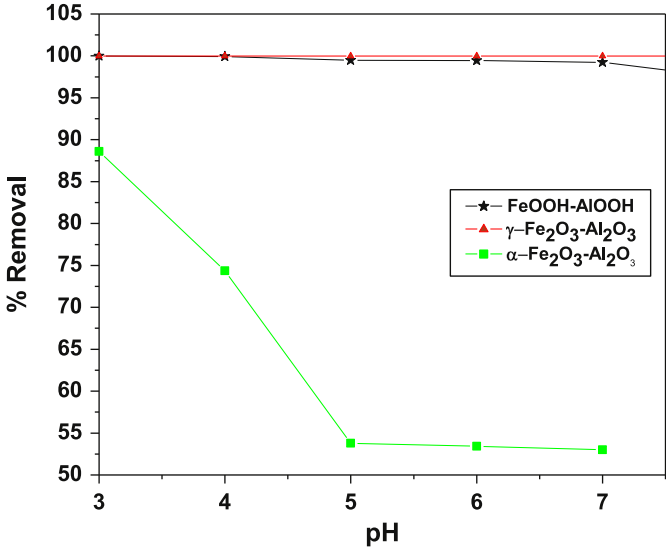

Fig. 6. Effect of pH on percentage removal of the Congo red dye.

the range of pH for Congo red adsorption was kept in the range of 3 to 8. The pH of the solution was adjusted by using 0.01 mol/L HCl or NaOH solutions. The graph of Congo red adsorbed with change in pH of the solution is shown in Fig. 6. From the figure it was observed that the percent removal of Congo red, has no effect on the pH of the solution and therefore we have carried out all the adsorption experiment at neutral pH 7. It was also observed that percentage removal of Congo red by both sintered and un-sintered samples with different pH have almost same values. But the sample sintered at 1000 °C showed less removal percent as compared to the oxy-hydroxy sample and the sample sintered at 500 °C. FeOOH–AlOOH nanocomposite shows better adsorption as compared to α-Fe_2O_3–Al_2O_3, it can be explained that there is an interaction of oxy-hydroxide group of nano-composite with the amine functional group of Congo red molecules, which brings out larger adsorption capacity [19]. Zhua et al. studied that Congo red anions in acidic and neutral solutions were easily adsorbed to Fe_3O_4 with positive surface charge but at higher pH values, Congo red anions were generally excluded away from the negatively charged surface of adsorbent, thus decreasing in percent removal of Congo red [20].

3.3.2. *Effect of contact time on adsorption study on Congo red dye*

The effect of contact time on the adsorption of Congo red was studied to determine the time taken by samples to remove 100 mg/L Congo red solutions. 0.1 g of the sample was added into a 10 mL of 100 mg/L Congo red solution. The variation of Congo red adsorbed with time is shown in Fig. 7. It was observed from the figure that the adsorption of Congo red by fixed amount of γ-Fe_2O_3–Al_2O_3 (sintered at 500 °C) nanocomposite increases with increase in time and the adsorption equilibrium is attained after 15 min contact time. This is because, a large number of vacant surface sites were available for adsorption during initial stage. However, with a lapse of adsorption time, the remaining vacant surface sites were difficult to be occupied due to repulsive forces between Congo red adsorbed on the surface of sample [20,21]. The concentration of Congo red in the solution was measured spectrophotometrically at 498 nm. The decrease in concentration of Congo red with time determines its adsorption onto the adsorbent surface. It was observed that within 15 min contact time, there was 100% removal of Congo red shown by both the oxy-hydroxide nanocomposite and the gamma mixed oxide nanocomposites. But in case of mixed α-Fe_2O_3–Al_2O_3 the adsorption capacity decreases as this is associated with loss

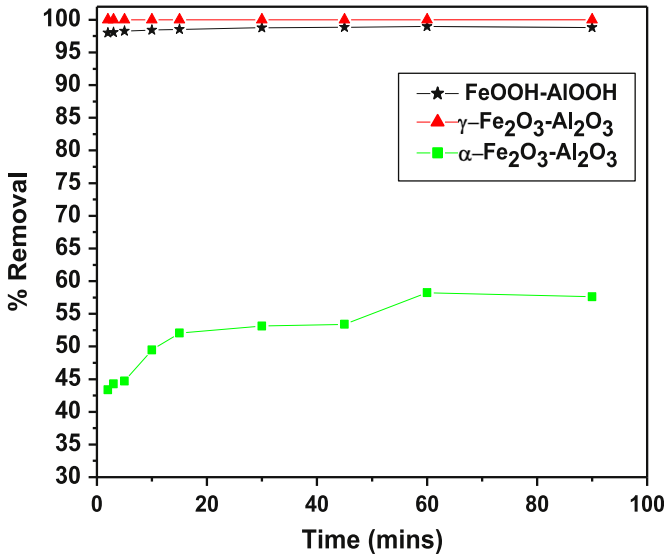

Fig. 7. Effect of contact time on removal of the Congo red dye.

of water of hydration and oxy-hydroxyl group in the crystalline structure. Thus mixed γ-Fe_2O_3–Al_2O_3 and oxy hydroxide of Iron and aluminum nanocomposite showed better adsorption as compared to α-Fe_2O_3–Al_2O_3 mixed nanocomposite.

3.3.3. *Effect of initial concentration on adsorption study of Congo red dye*

The variation of Congo red adsorbed with concentration of the solution is shown in Fig. 8. It was observed from this figure that, the percent removal of Congo red onto the as prepared FeOOH–AlOOH and γ-Fe_2O_3–Al_2O_3 nanocomposites is maximum and the value remain unaltered with increase in concentration of Congo red. It is also observed that within very short span of contact time both cases the adsorption attain the equilibrium value. It may be due to Congo red can absorb onto the metal oxide surface by coordination effect between metal ions and amine groups at the ends of Congo red molecules [22,23]. In case of mixed γ-Fe_2O_3–Al_2O_3 nanocomposites possesses water of hydration which form complexation via hydrogen bonding between the hydroxyl group and amine group of Congo red molecule for better adsorption of dye molecules on the surface. After sintering at higher temperatures the metastable γ- Fe_2O_3–Al_2O_3 phase gets converted into α-Fe_2O_3–Al_2O_3 and the removal capacity decreases as the availability of binding sites decreases as compared to that of oxy-hydroxy form and gamma mixed oxide. Thus among the three adsorbent materials γ-Fe_2O_3–Al_2O_3 can be considered as the most efficient adsorbent.

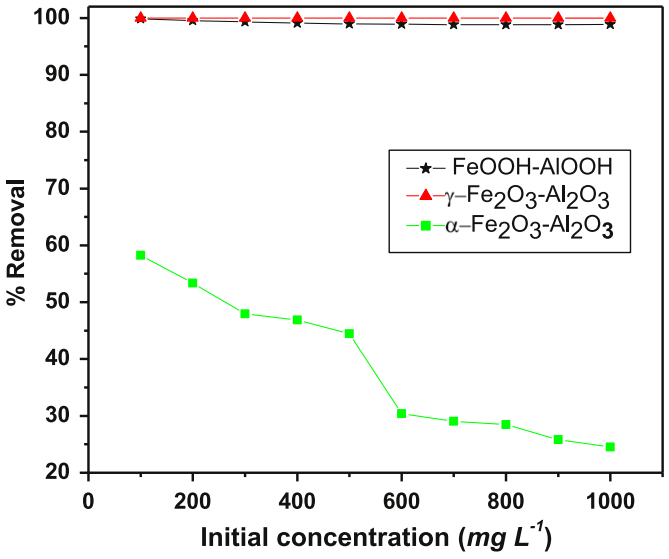

Fig. 8. Effect of initial concentration on percentage removal of the Congo red dye.

We have also studied the dye removal capacity and rate of adsorption by varying the adsorbent doses. In case of Congo red removal onto metal oxide surfaces, electrostatic attraction is the cause behind adsorption [24,25], but when the amount of dye is more and the dose increases, the unsaturated bonds get agglomerated within itself, and removal takes place. So to get the exact value of highest removal capacity, minimum amount of dose is taken while other experimental conditions remain the same. Fig. 9 shows the adsorption rate by gamma mixed oxide nanocomposite in a solution of 10 mL and 100 mg/L of Congo red where mass of the sample is 0.002 g. Similarly the Congo red removal percentage becomes 100%, when the mass of adsorbent is 0.002 g where as it is less in case of adsorbent having 0.001 g (data not attached). The results are presented in Fig. 9. The rate of adsorption of Congo red markedly slowed down due to small amount of porous structure. But the adsorption capacity reached 498 mg/g for 0.002 g of adsorbent in 60 min, with a removal percentage of 90% of Congo red. For further confirmation we have kept the solution for overnight after 2 h of stirring. It was observed that the solution become clear and the deep red color adsorbent was settled down at the bottom of the beaker. Thus, based on the above experimental result, it is concluded that the physical adsorption is responsible for decolorization of the dye and the oxidative degradation may also plays a secondary role in the whole process [24].

3.3.4. *Adsorption isotherm study of Congo red dye*

To describe the adsorption behavior of Congo red onto the three different phases of Iron-alumina mixed oxide nanocomposite, we have studied adsorption isotherms. The isotherm studies were carried out by varying the initial concentration of Congo red from 100 to 1000 mg/L and maintaining the

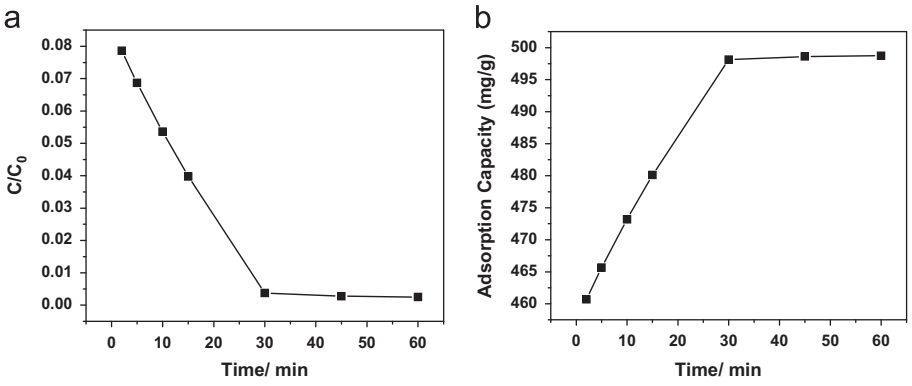

Fig. 9. (a) Adsorption rate and (b) adsorption capacities of a solution of Congo red (100 mg/L, 10 mL) where mass of the sample were 0.002 g.

adsorbent dosage of 0.1 g/L. An adsorption isotherm is an invaluable curve which describes the process governing the release or mobility of a substance from the aqueous porous media to a solid-phase at a constant temperature and pH [26]. The amount of dye adsorbed at equilibrium q_e (mg/g) was calculated from the following equation:

$$q_e = \frac{(C_0 - C_e)v}{m} \quad (1)$$

where C_0 (mg/L) is the initial dye concentration, Ce (mg/L) the equilibrium concentration of dye solution, v (L) the volume of dye solution, m (g) is the mass of adsorbent.

The equilibrium adsorption data obtained were analyzed using Langmuir and Freundlich isotherm models, which are represented by the following equations, respectively:

$$\frac{C_e}{q_e} = \frac{1}{bq_m} + \frac{C_e}{q_m} \quad (2)$$

$$q_e = K_f C_e^{1/n} \quad (3)$$

A linear form of the Freundlich isotherm can be obtained by taking logarithms of Eq. (3):

$$\log q_e = \log K_F + \log C_e \quad (4)$$

where q_m (mg/g) and b (L/mg) are Langmuir isotherm coefficients. The value of q_m represents the maximum adsorption capacity. K_f (mg/g) and n are Freundlich constants.

The Langmuir isotherm theory assumes monolayer coverage of adsorbate over a homogenous adsorbent surface and so the Freundlich isotherm is used to describe the surface heterogeneity of the sorbent [27,28]. It considers multilayer adsorption with a heterogeneous energetic distribution of active sites, accompanied by interactions between adsorbed molecules. Fig. 10 shows the Langmuir and Freundlich isotherm. Experiments on removal of Congo red dye by mixed oxide nanocomposites. The parameters of both the

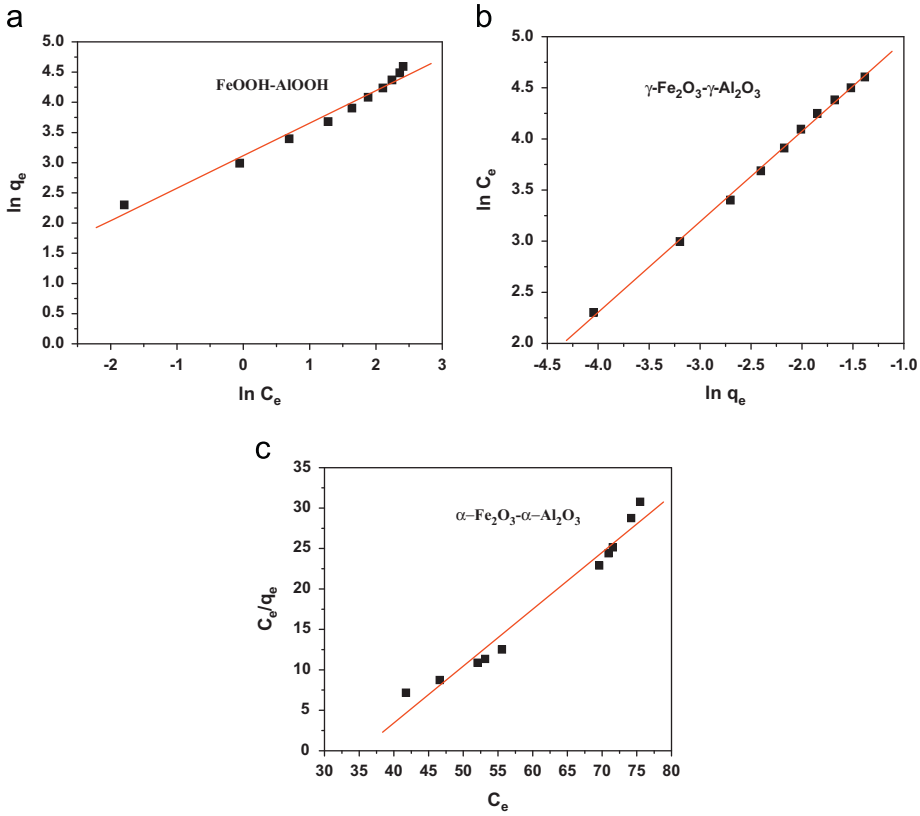

Fig. 10. Langmuir and Freundlich isotherm as obeyed of all the three different phases of Fe_2O_3–Al_2O_3 mixed oxide nanocomposite.

Table 1
Adsorption isotherm parameter of mixed oxide nanocomposite.

	Langmuir isotherm model			Freundlich isotherm model		
	q_m(mg/g)	b(L/mg)	R^2	K_F(mg/g)(L/mg)$^{1/n}$	n	R^2
FeOOH–AlOOH	126.58	5.696	0.793	22.42	1.85	0.976
γ-Fe_2O_3–γ-Al_2O_3	416.66	0.791	0.76	345.15	1.13	0.998
α-Fe_2O_3–α-Al_2O_3	1.422	0.061	0.968	100.34	−0.665	0.974

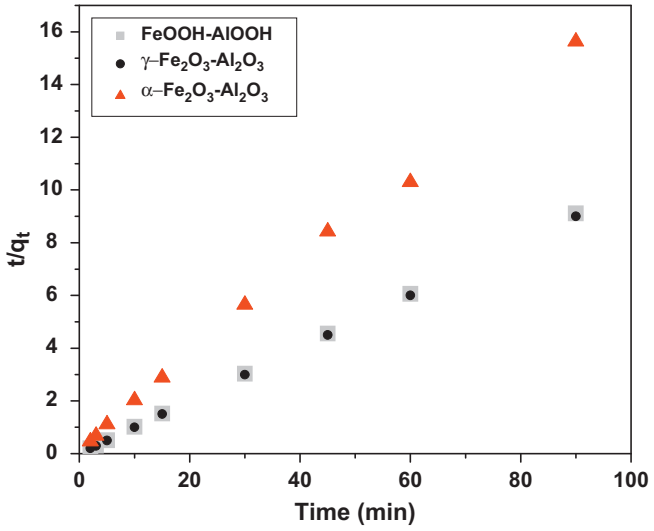

Fig. 11. Kinetic study of mixed oxide nanocomposite of three different phases.

isotherms data are listed in Table 1. Here we observed that, oxy-hydroxide phase obeys Freundlich isotherm more than Langmuir isotherm. Similarly, in the case of gamma mixed oxide nanocomposite it slightly obeys Langmuir and perfectly fits for Freundlich isotherm. But in case of α- Fe_2O_3–Al_2O_3 mixed oxide nanocomposite it obeys Langmuir isotherm.

3.3.5. *Adsorption kinetics study*

The applicability of the pseudo-first-order and pseudo-second-order model was tested for the adsorption of Congo red onto the three different phases of mixed oxide nanocomposites. The best fit model was selected according to the linear regression correlation coefficient, R^2 value. Here from the graph Fig. 11 it is clear that only pseudo-second -order kinetics is possible for all the three phases mixed oxide nanocomposite. The linearized form of pseudo-second-order rate equation is given as:

$$\frac{t}{q_t} = \frac{1}{k_2 q_e 2} + \frac{1}{q_e} t \tag{5}$$

where k_2 (g.(mg/min)) is the rate constant of the pseudo-second order equation. The value of q_e and k_2 can be determined by the slope and intercept of the straight line of the plot t/q_t versus t, respectively. Fig. 11 shows the sorption kinetics of Congo red onto mixed oxide nanocomposite surface obtained by batch experiments for an initial Congo red concentration of 100 mg/L at pH 7.0. The regression coefficient value (i.e., $R^2=1$ approximately), in every case confirmed the adsorption obeys pseudo-second order kinetics.

4. Conclusion

The mixed iron oxide–alumina nanocomposites have been synthesized using hydrothermal method. Batch experiments were performed for the removal of Congo red dye from aqueous solution, using three different phases of mixed oxide nanocomposite as adsorbent materials. Adsorption study was carried out by changing different parameters such as effect of time, pH and solution concentrations. Adsorption equilibrium is attained within a short contact time of 15 min. The adsorption capacity was found to be 498 mg/g approximately in case of gamma mixed oxides. The order of Congo red adsorption was governed by pseudo-second-order kinetics. The mixed nanocomposites obeyed Freundlich isotherm model as compared to Langmuir isotherm. Among the obtained nanocomposites gamma phase can act as a very good adsorbent for the 100% removal of Congo red.

Acknowledgement

The authors would like to acknowledge, DST Govt. of India for research funding.

References

[1] F. Hussain, M. Hojjati, M.O. kamoto, R.E. Gorga, Review article: polymer-matrix nanocomposites, processing, manufacturing, and application: an overview, Journal of Composite Materials 40 (2006) 1511–1559.
[2] I.S. Chronakis, Novel nanocomposites and nanoceramics based on polymer nanofibers using electrospinning process—a review, Journal of Materials Processing Technology 167 (2005) 283–293.
[3] S.R. Davis, A.R. Brough, A. Atkinson, Formation of silica/epoxy hybrid network polymers, Journal of Non-Crystalline Solids 315 (2003) 197–205.
[4] X. Wang, X. Kong, H. Zhang, Synthesis and characterization of water-soluble and bifunctional ZnO–Au nanocomposites, Journal of Physical Chemistry C 111 (2007) 3836–3841.
[5] H. Dong, M. Xie, J. Xu, M. Li, L. Peng, X. Gue, W. Ding, Iron oxide and alumina nanocomposite applied to Fischer–Tropsch synthesis, Chemical Communications 47 (2011) 4019–4021.
[6] K. Wu, T. Liu, W. Xue, X. Wang, Arsenic(III) oxidation/adsorption behaviors on a new bimetal adsorbent of Mn-oxide-doped Al oxide, Chemical Engineering Journal 192 (2012) 343–349.
[7] Y. Masue, R.H. Loeppert, T.A. Kramer, Arsenate and arsenite adsorption and desorption behavior on co-precipitated aluminum: iron hydroxides, Environmental Science and Technology 41 (2007) 837–842.
[8] A. Violante, M. Ricciardella, M. Pigna, Water, Adsorption of heavy metals on mixed Fe–Al oxides in the absence or presence of organic ligands, Air and Soil Pollution 145 (2003) 289–306.
[9] M.S. Chiou, P.Y. Ho, H.Y. Li, Adsorption of anionic dyes in acid solutions using chemically cross-linked chitosan beads, Dyes and Pigments 60 (2004) 69–84.
[10] L. Wang, A. Wang, Removal of Congo red from aqueous solution using a chitosan/ organomontmorillonite nanocomposite, Journal of Chemical Technology and Biotechnology 82 (2007) 711–720.
[11] S. Chatterjee, M.W. Lee, S.H. Woo, Adsorption of Congo red by chitosan hydrogel beads impregnated with carbon nanotubes, Bioresource Technology 101 (2010) 1800–1806.
[12] T.H. Kim, C. Park, J. Yang, S. Kim, Comparison of disperse and reactive dye removals by chemical coagulation and Fenton oxidation, Journal of Hazardous materials B 112 (2004) 95–103.
[13] S.J. Darzi, A.R. Mahjoub, Investigation of phase transformations and photocatalytic properties of sol–gel prepared nanostructured ZnO/TiO_2 composites, Journal of Alloys and Compounds 486 (2009) 805–808.

[14] J.L. Gong, B. Wang, G.M. Zeng, C.P. Yang, C.G. Niu, Q.Y. Niu, W.J. Zhou, Y. Liang, Removal of cationic dyes from aqueous solution using magnetic multi-wall carbon nanotube nanocomposite as adsorbent, Journal of Hazardous materials 164 (2009) 1517–1522.
[15] M.V. Kharlamova, N.A. Sapoletova, A.A. Eliseev, A.V. Lukashin, Optical properties of g-Ferric oxide nanoparticles in a mesoporous silica matrix, Technical Physics Letters 34 (2008) 288–291.
[16] J. Gangwar, K.K. Dey, Komal, Praveen, S.K. Tripathi, A.K. Srivastava, Microstructure, phase formations and optical bands in nanostructured alumina, Advanced Materials Letters 6 (2011) 402–408.
[17] B. Acemioglu, Adsorption of Congo red from aqueous solution onto calcium-rich fly ash, Journal of Colloid and Interface Science 274 (2004) 371–379.
[18] B. Wang, H. Wu, L. Yu, R. Xu, T.T. Lim, X.W. Lou, Template-free formation of uniform urchin-like α-FeOOH hollow spheres with superior capability for water treatment, Advanced Materials 24 (2012) 1111–1116.
[19] J. Fei, Y. Cui, J. Zhao, L. Gao, Y. Yang, J. Li, Large-scale preparation of 3D self-assembled iron hydroxide and oxide hierarchical nanostructures and their applications for water treatment, Journal of Materials Chemistry 21 (2011) 11742.
[20] H.Y. Zhua, Y.Q. Fu, R. Jiang, J.H. Jiang, L. Xiao, G.M. Zeng, S.L. Zhao, Y. Wang, Adsorption removal of Congo red onto magnetic cellulose/Fe_3O_4/activated carbon composite: equilibrium, kinetic and thermodynamic studies, Chemical Engineering Journal 173 (2011) 494–502.
[21] W. Cai, Y. Hu, J. Chen, G. Zhang, T. Xia, Synthesis of nanorod-like mesoporous -Al_2O_3 with enhanced affinity towards Congo red removal: Effects of anions and structure-directing agents, Crystal Engineering Communication 14 (2012) 972–977.
[22] M.M. Abd El-Latif, A.M. Ibrahim, M.F. El-Kady, Adsorption equilibrium, kinetics and thermodynamics of methylene blue from aqueous solutions using biopolymer oak sawdust composite, Journal of American science 6 (2010) 267–283.
[23] C. Yu, X. Dong, L. Guo, J. Li, F. Qin, L. Zhang, J. Shi, D. Yan, Template-free preparation of mesoporous Fe_2O_3 and its application as absorbents, Journal of Physical Chemistry C 112 (2008) 13378–13382.
[24] X.H. Lu, D.Z. Zheng, J.Y. Gan, Z.Q. Liu, C.L. Liang, P. Liu, Y.X. Tong, Porous CeO_2 nanowires/nanowire arrays: electrochemical synthesis and application in water treatment, Journal of Materials Chemistry 20 (2010) 7118–7122.
[25] P.X. Huang, F. Wu, B.L. Zhu, X.P. Gao, H.Y. Zhu, T.Y. Yan, W.P. Huang, S.H. Wu, D.Y. Song, CeO2 nanorods and gold nanocrystals supported on CeO2 nanorods as catalyst, Journal of Physical Chemistry B 109 (2005) 19169–19174.
[26] G. Limousin, J.P. Gaudet, L. Charlet, S. Szenknect, V. Barthe's, M. Krimissa, Sorption isotherms: a review on physical bases, modeling and measurement, Applied Geochemistry 22 (2007) 249–275.
[27] E. Bulut, M. Ozacar, I.A. Sengil, Equilibrium and kinetic data and process design for adsorption of Congo red onto bentonite, Journal of Hazardous materials 154 (2008) 613–622.
[28] S.J. Allen, G. Mckay, J.F. Porter, Adsorption isotherm models for basic dye adsorption by peat in single and binary component systems, Journal of Colloid and Interface Science 280 (2004) 322–333.